IEEE Access
Multidisciplinary | Rapid Review | Open Access Journal

Received November 21, 2019, accepted December 15, 2019, date of publication December 19, 2019, date of current version December 31, 2019.

Digital Object Identifier 10.1109/ACCESS.2019.2960832

A Novel Emotion Control System for Embedded Human–Computer Interaction in Green Iot

CHAO GONG[1], **FUHONG LIN**[1], **AND XINGSHUO AN**[2]
[1]School of Computer and Communication Engineering, University of Science and Technology Beijing, Beijing 100083, China
[2]North China Institute of Computing Technology, Beijing 100083, China

Corresponding author: Fuhong Lin (fhlin@ustb.edu.cn)

This work was supported in part by the National Science Foundation Project of China under Grant 61931001 and Grant 61873026, and in part by the National Key Research and Development Program of China under Grant 2017YFC0820700.

ABSTRACT The green Internet of Things (IoT) technology has increased the need for a more emotion-connected human-computer interaction. The lower network latency and longer battery life ensure the continuous and real-time work of human-computer interaction systems in embedded environments. However, the lack of emotional dynamics limits the empathy capability of human-computer interactions. In this paper, we propose a novel emotion control system for embedded human-computer interaction in green IoT. The Van Der Pol emotional dynamics with nonlinear resilience is proposed for the modeling of human emotional mechanisms. Moreover, respectively for the autonomous and stochastic-excitation situation, we analyze the stability of the solution, based on which four kinds of the emotional health status are defined. Finally, we obtain the steady-state solution and design its feedback controller. Results of the numerical simulation and prototype demonstrate the validity and practical operability of the theory.

INDEX TERMS Green IoT, emotion control, emotional dynamics, Van Der Pol oscillator, human-computer interaction.

I. INTRODUCTION

The power of cloud computing and the massive scale of big data have made the success of artificial intelligence (AI) [1], [2], in a manner of high performance computing and high power consumption. However, with the emergence of edge computing [3] and the rise of green Internet of Things (IoT) technology [4], the core of AI is gradually sinking from the cloud to the user's closer end [5]. The lower latency [6] and longer battery [7] life of the green IoT network has spawned the new demand for a more advanced artificial intelligence capable of empathy in some embedded environments with strong human interaction [8]. Applying green IoT techniques [9] to the controllable human-computer interaction to achieve an emotion-friendly green IoT will be an important technological upgrade and industrial revolution in the fusion of IoT and AI.

Empathy is the core of human-computer interaction, including both the positive recognizability [10] and the reverse controllability [11] of emotions. Emotion recognition has always been a hot topic for research. Different emotional representations, such as speech, facial expression and physiological signals, are collected to characterize and measure the category and intensity of emotions and a series of satisfactory results have been achieved [12]. However, emotion control has always been an unsolved problem in the research of human-computer interaction, which is due to the following three reasons.

- The control response has to be low-latency to meet the timeliness requirements, which can not be satisfied by the cloud ''brain''.
- Emotion control requires a rich means of stimulating or interfering with human senses.
- The first condition for a system to be controlled is to grasp its dynamics, which is precisely unfinished in current emotional researches.

The edge computing paradigm provides low latency computing services around the user [13], enabling the first problem to be solved now. The full range of human sensory coverage brought by the IoT's broader embedded applications [14] (such as the sound, lighting, temperature in smart homes [15] and the speed, driving intensity, music in autonomous vehicles [16], etc.) and the energy security for its green revolution [17] makes the second problem no longer

The associate editor coordinating the review of this manuscript and approving it for publication was Zhenyu Zhou.

exist. However, the lack of intrinsic dynamics of human emotions has still not been resolved.

In this paper, we propose a novel emotion control system for embedded human-computer interaction in green IoT to achieve mathematical modeling, stability analysis and feedback control of human emotions. First, we establish a Van Der Pol emotional dynamics model with nonlinear resilience based on human emotional characteristics. Then, we analyze the trajectory stability of the model in the autonomous situation and define the emotional health state, including *Stable State*, *Gradual Dead State*, *Dead State* and *Explosion State*. Finally, we discuss the steady-state response of the emotional dynamic model in the case of random excitation (broadband Gaussian white noise), and design the feedback controller based on the steady-state solution of the emotional state displacement and the transfer velocity.

The remainder of the paper is organized as follows. In Section II, we summarize the related work. In Section III, an emotional dynamics model with nonlinear resilience was proposed. In Section IV, the stability of the model under autonomous conditions is analyzed, and the health state of emotions is defined. In Section V, we discuss the stability performance of the model in the face of stochastic excitations and design a feedback controller to maintain its stability. The results of numerical simulation and prototype are reported in Section VI, followed by the conclusion.

II. RELATED WORK

In the field of psychology research, there are many studies on emotional regulation. Kraaij and Garnefski [18] studied the psychometric properties of the Behavioral Emotion Regulation Questionnaire (BERQ) and its relationship with well-being. The results show the importance of subject behavior control in psychological intervention strategies. Brett Q. Ford *et al.* [19] studied the effects of emotion revaluation on negative emotion control and explored the use of this outcome in the US election to control voter political behavior. Williams *et al.* [20] demonstrated the importance of the Interpersonal Emotion Regulation (IER) in emotional regulation through a study of the social network of the new dormitory and found the independence between different emotions. Although there have been many years of experience in the study of emotional control from a psychological perspective, it is difficult to obtain practical application in human-computer interaction and machine emotion control.

In the practical application of human-computer emotional interaction and emotional regulation, researchers are more likely to evaluate the emotional state through some external observable and quantitative information. If certain features of the information will result in negative emotions, we can achieve the purpose of emotion control by artificially changing the external environment created by the feature. Elhai *et al.* [21] explored the relationship between human emotional state and the use frequency of smartphones, and designed an emotional adjustment strategy by controlling the use time of smartphones. Haines *et al.* [22] combined computer vision and machine learning to encode facial expressions in real time and studied the emotional effects of facial expressions on receptors. Villani *et al.* [23] evaluated and studied using video games as a treatment tool for patients with emotional disorders such as depression, and exerted emotional interventions on patients through different gaming experiences. These methods have achieved the purpose of emotional intervention to a certain extent. However, the internal principle of emotion is always unknown, and all these work can only be regarded as external clues, which makes it difficult to accurately and effectively control emotions.

In order to achieve control over human emotions, it is necessary to have an in-depth understanding of the operational mechanisms of emotions, or the emotional dynamics. Bringmann *et al.* [24] modeled the emotional system based on a parametric time-varying vector-autoregressive model (TV-VAR) to simulate the temporal dependence of emotions and to demonstrate the availability of the system. Krone *et al.* [25] proposed a vector autoregressive Bayesian sentiment dynamics model to predict the basic emotions with long-term dependence based on short time sequences. Jenke and Peer [26] used dynamic field theory, combined with theoretical knowledge and data-driven experimental methods, to model the dynamic characteristics of emotions, deepening the understanding of emotional mechanisms. The above research fully exploited the time-dependent attributes of emotions and modeled the emotional system as a shock-recovery model with some steady-state characteristics. However, the stability of emotions is not a simply unchanged state, but an orbital stability [27]. The above-mentioned hypothetical model cannot simulate the periodic oscillation of the emotional state. Moreover, there is no further attempt to explore the stability control problem.

III. THE VAN DER POL EMOTIONAL DYNAMICS MODEL WITH NONLINEAR RESILIENCE

Based on years of research in biopsychology and brain science, we know that brain emotions have the following dynamic characteristics: 1.

1) The emotional state oscillates according to a certain period, rather than being static. Even if it is not subject to external shocks, the emotional state will still fluctuate constantly [28].
2) After an external shock, the emotional system can always return to a stable orbit [29].
3) The recovery of the emotional state is not linear and the recovery rate is not constant, indicating that it has nonlinear resilience [30].

According to the first and second features above, we model the emotional displacement state x based on the Van der Pol equation [31].

$$\ddot{x} - (\mu - x^2)\dot{x} + \omega_0^2 x = F(t), u \in \boldsymbol{R}^1 \tag{1}$$

where $F(t)$ is the external emotional stimulus, $-(\mu - x^2)\dot{x}$ is the damping term of the emotional dissipative system, μ

is the environmental parameter and $\omega_0^2\, x$ is the resilience item of the emotional recovery system. When x or $\ddot{x}$ is small, the damping term is negative. In the opposite case, the damping term is positive. When $F(t)$ is zero, the system will automatically adjust to stable vibration according to the initial state. When $F(t)$ is not zero, the system's resilience will return the system to stable vibration. The particularity of the Van der Pol vibration is that its phase trajectory in the phase plane is an isolated closed curve (limit cycle). The corresponding periodic motion is uniquely determined by the physical parameters of the system, independent of the initial state. It is worth noting that the Van der Pol system does not meet the stability conditions of Lyapunov, but the orbit is stable, satisfying the Poincaré stability.

According to the third feature of the emotional system, we replace the linear recovery item $\omega_0^2\, x$ in Eq. (1) with a nonlinear function $g(x) = \omega_0^2\, x + \mu x^2 + \mu x^3$ and get

$$\ddot{x} - (\mu - x^2)\dot{x} + g(x) = F(t), u \in \boldsymbol{R}^1. \tag{2}$$

Next, we will analyze the stability of the emotional dynamic system under different external stimulus situations and propose corresponding stability control strategies.

IV. STABILITY AND HEALTH STATUS OF EMOTIONAL SYSTEM IN AUTONOMOUS SITUATIONS

In the autonomous situation, the external input of the system is $F(t) = 0$, and the state equation of the system is

$$\ddot{x} - (\mu - x^2)\dot{x} + \omega_0^2 x + \mu x^2 + \mu x^3 = 0, u \in \boldsymbol{R}^1. \tag{3}$$

Introducing state variables $x_1 = x$, $x_2 = \dot{x}$, Eq. (3) transforms into a state equation form

$$\begin{aligned}\dot{\boldsymbol{x}} &= [\dot{x_1}\ \dot{x_2}]^{\mathrm{T}} \\ &= \begin{bmatrix} x_2 \\ \omega_0^2 x_1 + (\mu - x_1^2)x_2 - \mu x_1^2 - \mu x_1^3 \end{bmatrix} \\ &= f(\boldsymbol{x}, \mu).\end{aligned} \tag{4}$$

We can get

$$f(\boldsymbol{0}, \mu) = 0, \quad \forall \mu \in \boldsymbol{R}^1 \tag{5}$$

where $\dot{\boldsymbol{x}} = 0$ when $\boldsymbol{x} = 0$ indicating that 0 solution is the equilibrium point of the system.

If the 0 solution of the emotional system described by Eq. (4) is stable, it means that the system will remain silent regardless of the initial state or whatever emotional stimulus is applied, which is called the dead emotion system. On the contrary, when the 0 solution is unstable, we will study whether there are other stable solutions.

Eq. (4) can be expressed as

$$\dot{\boldsymbol{x}} = \begin{bmatrix} 0 & 1 \\ -\omega_0^2 & \mu \end{bmatrix}\begin{bmatrix} x_1 \\ x_2 \end{bmatrix} + \begin{bmatrix} 0 \\ -x_1^2 x_2 - \mu x_1^2 - \mu x_1^3 \end{bmatrix}. \tag{6}$$

Take the first-order approximation equation Jacobian matrix as

$$\boldsymbol{A}(\mu) = D_{\boldsymbol{x}}\boldsymbol{f}(0, \mu) = \begin{bmatrix} 0 & 1 \\ -\omega_0^2 & \mu \end{bmatrix},$$

and

$$\boldsymbol{g}(\boldsymbol{x}, \mu) = \begin{bmatrix} g_1(\boldsymbol{x}, \mu) \\ g_2(\boldsymbol{x}, \mu) \end{bmatrix} = \begin{bmatrix} 0 \\ -x_1^2 x_2 - \mu x_1^2 - \mu x_1^3 \end{bmatrix}.$$

Then, according to

$$|\lambda \boldsymbol{E} - \boldsymbol{A}| = \begin{bmatrix} 0 & -1 \\ \omega_0^2 & \lambda - \mu \end{bmatrix} = 0\ ,$$

we can get the characteristic equation of matrix $\boldsymbol{A}$ as

$$\lambda^2 - \lambda\mu + \omega_0^2 = 0.$$

We have

$$\Delta = \mu^2 - 4\omega_0^2,$$

and the conjugate eigenvalues when $|\mu| < 2\omega_0$

$$\lambda_{1,2}(\mu) = \frac{\mu \pm i\sqrt{-\Delta}}{2} = \alpha(\mu) \pm i\beta(\mu). \tag{7}$$

When $\Delta \geq 0, |\mu| \geq 2\omega_0$, there is no central manifold in the system. The nonlinear term $\boldsymbol{g}(\boldsymbol{x}, \mu)$ of the system has a weak influence on the phase trajectories outside the central manifold. At this point, we can directly analyze its corresponding first approximation equation to study the system Eq. (4).

$$\dot{\boldsymbol{x}} = \boldsymbol{A}\boldsymbol{x}. \tag{8}$$

According to the theory of first-order linear differential equations, λ_1 and λ_2 are negative when $\mu \leq 0$. The system only has a stable manifold and the 0 solution (equilibrium point) is a stable node. Such emotional systems will quickly decay to the equilibrium point (0 solution) regardless of the initial state or external incentives. We call this kind of emotional system state the *Dead state*, which is dangerous and a healthy emotional system should avoid.

When $\mu > 0, \lambda_1$ and λ_2 are both positive. There is no stable manifold in the system, and the 0 solution (equilibrium point) is an unstable node. Such emotional systems will quickly produce self-oscillation away from the equilibrium point until the emotional explosion. We call this kind of emotional system state the *Explosion State*, which can result in irreversible damage.

When $\Delta < 0$ and $|\mu| < 2\omega_0$, λ_1 and λ_2 are conjugate roots and

$$\alpha(0) = 0, \beta(0) = \omega_0 > 0, c = \frac{\mathrm{d}\alpha}{\mathrm{d}\mu}|_{\mu=0} = \frac{1}{2} > 0. \tag{9}$$

According to the two-dimensional Hopf bifurcation theorem [32], the equilibrium point of the equation Eq. (4) loses stability at $\mu = 0$ because the system satisfies the condition Eqs. (5), (7) and (9). And when $ac\mu < 0$, the system appears Hopf bifurcation, and its stability (depending on whether a stable limit cycle can occur) is opposite to that of the equilibrium point.

$$a(\mu) = \frac{1}{16}\left(\frac{\partial^3 f}{\partial x_1^3} + \frac{\partial^3 f}{\partial x_1 \partial x_2^2} + \frac{\partial^3 g}{\partial x_1^2 \partial x_2} + \frac{\partial^3 g}{\partial x_2^3}\right)$$

$$+\frac{1}{16\omega_0}\left[\frac{\partial^2 f}{\partial x_1 \partial x_2}\left(\frac{\partial^2 f}{\partial x_1^2}+\frac{\partial^2 f}{\partial x_2^2}\right)-\frac{\partial^2 g}{\partial x_1 \partial x_2}\left(\frac{\partial^2 g}{\partial x_1^2}+\frac{\partial^2 g}{\partial x_2^2}\right)-\frac{\partial^2 f}{\partial x_1^2}\frac{\partial^2 g}{\partial x_1^2}+\frac{\partial^2 f}{\partial x_2^2}\frac{\partial^2 g}{\partial x_2^2}\right]$$
$$=-\frac{1}{8}-\frac{2x_1x_2+2\mu x_1+6\mu x_1^2}{8\omega_0}$$

$a=a(0)=-\frac{1}{8}$ when $(x_1, x_2, \mu)=(0,0,0)$.

The system has a stable limit cycle with an average radius $\tilde{r}$ and an angular frequency $\tilde{\omega}$.

$$\tilde{r}=2\mu^{1/2}. \tag{10}$$
$$\tilde{\omega}=(\omega_0^2-\mu/4)^{1/2}. \tag{11}$$

Therefore, when $\mu < 0$, no bifurcation occurs and the equilibrium point is the stable focus. The system will go to 0 solution inexhaustibly, and we call this emotional system state the *Gradual Dead State*. The gradual dead state is desensitized and the system is no longer sensitive to any incentives. It is a dangerous sign that the system reaches the gradual dead state.

When $\mu \geq 0$, the system produces a bifurcation and a stable limit cycle is generated. The equilibrium point is the stable center. The system has a periodic solution and is in constant amplitude self-excited oscillation. The system will adjust itself to the steady-state self-excited vibration regardless of the initial state or external excitation. We call this emotional system state the *Stable State*, which is healthy.

In summary, we get

$$\begin{cases}\mu \leq -2\omega_0 & \textit{Dead State}\\ -2\omega_0<\mu<0 & \textit{Gradual Dead State}\\ 0\leq\mu<2\omega_0 & \textit{Stable State}\\ \mu\geq 2\omega_0 & \textit{Explosion State}\end{cases} \tag{12}$$

V. STEADY-STATE RESPONSE ANALYSIS AND STABILITY CONTROL WITH BROADBAND GAUSSIAN WHITE NOISE EXCITATIONS

The undisturbed environment does not exist in reality and the emotional system is always subject to stochastic external excitations. The stochastic steady-state response research has more practical significance. Typically, external noises of the affective system are substantially uniform stochastic signals with a significantly greater frequency bandwidth than the emotional system. The relaxation time of the emotional system is significantly larger than the correlation time of stochastic excitations, which can be approximated as Gaussian white noises and

$$E[F(t)]=0,$$
$$S_F(\omega)=K,$$
$$E[F(t)F(t-\tau)]=2\pi K,$$
$$F(t)=\sqrt{2\pi K}N(t),$$

in which $N(t)$ is the Gaussian white noise of unit intensity.

When the system is excited by a stochastic stimulus $F(t)$, the system state equation can be expressed as

$$\ddot{x}+\varepsilon^2 h(x)\dot{x}+g(x)=\varepsilon F(t), \tag{13}$$

where $h(x)$ is the damping function, and

$$h(x)=x^2-\mu,$$

$g(x)$ is the nonlinear resilience function

$$g(x)=w_0^2x+\mu x^2+\mu x^3.$$

ε is a small parameter and $0<\varepsilon\ll 1$. To make the system's response limited, the power consumed by the damping should be of the same order of magnitude as the power of the stochastic excitation. So the damping term is proportional to ε^2, and the stimulus is proportional to ε. To convert the equation into a standard form of differential equation, we take the energy envelope (total energy) of the system as

$$E(t)=\frac{1}{2}\dot{x}^2+V(x), \tag{14}$$

in which

$$V(x)=\int_0^x g(\xi)d\xi.$$

Take the transformation

$$\begin{cases}V(x)=E\cos^2\Phi\\ \dot{x}=-\sqrt{2E}\sin\Phi\end{cases} \tag{15}$$

and according to the first equation in Eq. (15), we get

$$\dot{E}=\frac{2V(x)\sin\Phi}{\cos^3\Phi}\dot{\Phi}-\frac{\sqrt{2E}g(x)\sin\Phi}{\cos^2\Phi}, \tag{16}$$

which can also be expressed as

$$\dot{\Phi}=\frac{\cos^3\Phi}{2V(x)\sin\Phi}\dot{E}+\frac{\sqrt{E}g(x)\cos\Phi}{\sqrt{2}V(x)}. \tag{17}$$

From the second equation in Eq. (15), we get

$$\ddot{x}=-\frac{\sin\Phi}{\sqrt{2E}}\dot{E}-\sqrt{2E}\cos\Phi\dot{\Phi}. \tag{18}$$

Substituting Eq. (13) into Eq. (18), there is

$$-\frac{\sin\Phi}{\sqrt{2E}}\dot{E}-\sqrt{2E}\cos\Phi\dot{\Phi}=\varepsilon^2\sqrt{2E}h\sin\Phi-g(x)+\varepsilon y(t). \tag{19}$$

Substituting Eqs. (16) and (17) into Eq. (19), the system state equation can be transformed into first order differential equations as

$$\dot{E}=\alpha_1(E,\Phi)+\beta_1(E,\Phi)F(t), \tag{20}$$
$$\dot{\Phi}=\alpha_2(E,\Phi)+\beta_2(E,\Phi)F(t), \tag{21}$$

in which

$$\alpha_1(E,\Phi)=-\varepsilon^2\cdot 2Eh\sin^2\Phi,$$
$$\alpha_2(E,\Phi)=\varepsilon^2\cdot h\sin\Phi\cos\Phi+\frac{|g(x)|}{V(x)},$$

$$\beta_1(E,\Phi) = -\varepsilon\sqrt{2E}\sin\Phi,$$
$$\beta_2(E,\Phi) = -\varepsilon\frac{\cos\Phi}{\sqrt{2E}}.$$

Set the system state vector as

$$\boldsymbol{y} = [y_1\ y_2]^{\mathrm{T}} = [E\ \Phi]^{\mathrm{T}}, \tag{22}$$

and Eqs. (20) and (21) can be expressed as

$$\frac{\mathrm{d}}{\mathrm{d}t}\boldsymbol{y} = \boldsymbol{\alpha}(\boldsymbol{y},t) + \boldsymbol{\beta}(\boldsymbol{y},t)F(t). \tag{23}$$

Set

$$\boldsymbol{\beta}'(\boldsymbol{y},t) = \sqrt{2\pi K}\boldsymbol{\beta}(\boldsymbol{y},t),$$

and there is

$$\frac{\mathrm{d}}{\mathrm{d}t}\boldsymbol{y} = \boldsymbol{\alpha}(\boldsymbol{y},t) + \boldsymbol{\beta}'(\boldsymbol{y},t)N(t). \tag{24}$$

In addition, $N(t)$ can be regarded as the formal derivative of the unit Wiener process $W(t)$, which means

$$\mathrm{d}W(t) = N(t)\mathrm{d}t.$$

So we obtain

$$\mathrm{d}\boldsymbol{y} = \boldsymbol{\alpha}(\boldsymbol{y},t)\mathrm{d}t + \boldsymbol{\beta}'(\boldsymbol{y},t)\circ\mathrm{d}W(t), \tag{25}$$

in which $\circ$ represents the Stratonovich stochastic differential equation. After adding the Wong-Zakai correction, Eq. (25) can be transformed into the following *Itô* stochastic differential equation

$$\mathrm{d}\boldsymbol{y} = \boldsymbol{\alpha}'(\boldsymbol{y},t)\mathrm{d}t + \boldsymbol{\beta}'(\boldsymbol{y},t)\mathrm{d}W(t), \tag{26}$$

in which

$$\begin{aligned}\alpha_1' &= \alpha_1 + \pi\sum_j K\beta_j\frac{\partial}{\partial y_j}\beta_1\\ &= \varepsilon^2(-2\,Eh\sin^2\Phi + \pi K)\\ &\quad j=1,2\\ \alpha_2' &= \alpha_2 + \pi\sum_j K\beta_j\frac{\partial}{\partial y_j}\beta_2\\ &= \varepsilon^2(h - \frac{\pi K}{E})\sin\Phi\cos\Phi + \frac{|g(x)|}{V(x)}\\ &\quad j=1,2\end{aligned}$$

The Gaussian white noise $F(t)$ has a very small correlation time, while $\boldsymbol{y}(t)$ has a very large relaxation time equivalent to the magnitude of $[\frac{\partial\boldsymbol{\alpha}_j}{\partial\boldsymbol{y}_k}]^{-1}\propto\frac{1}{\varepsilon^2}$. Therefore, we can easily find a non-overlapping time interval with the length between the correlation time of $F(t)$ and the relaxation time of $\boldsymbol{y}(t)$. The $\boldsymbol{y}(t)$ observed at each discrete moment on the endpoints of these intervals will be an approximate Markov process. The FPK equation that its transition probability density satisfies can be obtained from the *Itô* equation Eq. (26), whose drift coefficient and diffusion coefficient are respectively

$$A_1(\boldsymbol{y},t) = \alpha_1'(\boldsymbol{y},t), \tag{27}$$
$$A_2(\boldsymbol{y},t) = \alpha_2'(\boldsymbol{y},t), \tag{28}$$
$$\begin{aligned}B_{11}(\boldsymbol{y},t) &= \beta_1'^2(\boldsymbol{y},t)\\ &= \varepsilon^2\cdot 4\pi KE\sin^2\Phi,\end{aligned} \tag{29}$$
$$\begin{aligned}B_{12}(\boldsymbol{y},t) &= \beta_1(\boldsymbol{y},t)\beta_2(\boldsymbol{y},t)\\ &= \varepsilon^2\cdot 2\pi K\sin\Phi\cos\Phi,\end{aligned} \tag{30}$$
$$B_{21}(\boldsymbol{y},t) = B_{12}(\boldsymbol{y},t), \tag{31}$$
$$\begin{aligned}B_{22}(\boldsymbol{y},t) &= \beta_2'^2(\boldsymbol{y},t)\\ &= \varepsilon^2\cdot\pi K\frac{\cos^2\Phi}{E}.\end{aligned} \tag{32}$$

The above process is the first step approximation of the stochastic averaging method.

The Eq. (20) indicates that E is a slow variable. The existence of $\frac{|g(x)|}{V(x)}$ in Eq. (21) makes Φ a fast variable. $\boldsymbol{\alpha}(\boldsymbol{y},t)$ and $\boldsymbol{\beta}(\boldsymbol{y},t)$ are both periodic functions of the fast variable Φ, so we can average them over a period by the fast variable. This is the second step approximation. The averaged state equation will not depend on Φ, which means that the system has achieved dimensionality reduction. The solution to the slow variable E can be used to approximate the solution of the original system.

The *Itô* stochastic differential equation for the one-dimensional Markov diffusion process E is

$$\mathrm{d}\boldsymbol{E} = \alpha_1'\mathrm{d}t + \beta_1'\mathrm{d}W(t). \tag{33}$$

After being averaged over a period of the fast variable Φ, the corresponding FPK equation has the drift coefficient $A_1(E,\Phi)$ and the diffusion coefficient $B_1(E,\Phi)$ as

$$\bar{A}_1(E) = \varepsilon^2(-2H(E) + \pi K), \tag{34}$$

in which

$$H(E) = \frac{1}{2\pi}\int_0^{2\pi} h(E,\Phi)\sin^2\Phi\mathrm{d}\Phi,$$

and

$$\begin{aligned}\bar{B}_{11}(E) &= \varepsilon^2\cdot 4\pi KE\cdot\frac{1}{2\pi}\int_0^{2\pi}\sin^2\Phi\mathrm{d}\Phi\\ &= \varepsilon^2\cdot 2\pi KE.\end{aligned}$$

The transition probability density of $E(t)$ satisfy

$$\frac{\partial p}{\partial t} = -\frac{\partial}{\partial E}[\bar{A}_1(E,t)p] + \frac{1}{2}\frac{\partial^2}{\partial E^2}[\bar{B}_{11}(E,t)p], \tag{35}$$

in which p represents $p(E,t|E_0,t_0)$.

In order to obtain the joint transition probability density of the displacement variable and velocity variable, we first calculate

$$p(x,E,t) = p(x,t|E)p(E,t),$$

where $p(x,t|E)$ represents the transition probability density of x for the given energy E. It is equal to the ratio of the time that the system displacement stays at x over the entire period $T(E)$ under the condition E.

$$p(x,t|E) = \frac{1}{T(E)\sqrt{2(E-V(x))}}.$$

So we have

$$p(x, E, t) = \frac{p(E, t)}{T(E)\sqrt{2(E - V(x))}}. \quad (36)$$

In order to find the time period $T(E)$ corresponding to the fast variable Φ over 2π, Eq. (14) indicates that

$$\mathrm{d}t = \pm\frac{\mathrm{d}x}{\sqrt{2(E - V(x))}}. \quad (37)$$

We integrate both sides and get

$$T(E) = 2\int_{\mathrm{R}} \frac{\mathrm{d}x}{\sqrt{2(E - V(x))}} = 2\sqrt{2}\int_0^b \frac{\mathrm{d}x}{\sqrt{E - V(x)}}, \quad (38)$$

where R represents the domain of x within a period of $T(E)$ and b means $V(b) = E$.

According to Eq. (14), the joint probability density of the displacement x and the velocity $\dot{x}$ can be obtained as

$$p(x, \dot{x}, t) = \frac{p(E, t)}{T(E)}\bigg|_{E=\frac{1}{2}\dot{x}^2+V(x)}. \quad (39)$$

Then we can get their edge probability density as

$$p(x, t) = \int_{-\infty}^{+\infty} p(x, \dot{x}, t)\mathrm{d}\dot{x}, \quad (40)$$

$$p(\dot{x}, t) = \int_{-\infty}^{+\infty} p(x, \dot{x}, t)\mathrm{d}x. \quad (41)$$

Since $F(t)$ is Gaussian white noise, $E(T)$ described by Eq. (35) is a one-dimensional temporally homogeneous diffusion process. When $t \to \infty$, $E(t)$ will tend to be a smooth diffusion process. Setting $\frac{\partial p}{\partial t} = 0$ and considering Eq. (35) for E's boundary condition $E = 0, p < \infty, E \to Infty, p \to 0, \frac{\partial p}{\partial t} \to 0$, we can integrate to get the steady-state probability density of $E(t)$ as

$$p(E) = \frac{C}{\bar{B}_{11}(E)} \exp\left[\int_0^E \frac{2\bar{A}_1(s)}{\bar{B}_{11}(s)} ds\right], \quad (42)$$

where C is the normalization constant. The steady-state probability density $p(x)$ of x can be obtained from Eqs. (39) and (40). The expected displacement state of the emotional system can be expressed as

$$E\{x\} = \int_{-\infty}^{+\infty} xp(x)dx. \quad (43)$$

In order to maintain the stability of the periodic solution when subjected to stochastic external excitations, we set up a feedback controller in the emotional system as

$$u = \varepsilon k_1(x - E\{x\}) + \varepsilon k_2(x - E\{x\})^3, \quad (44)$$

where k_1 and k_2 indicate the control gain and $E\{x\}$ indicates the expectation.

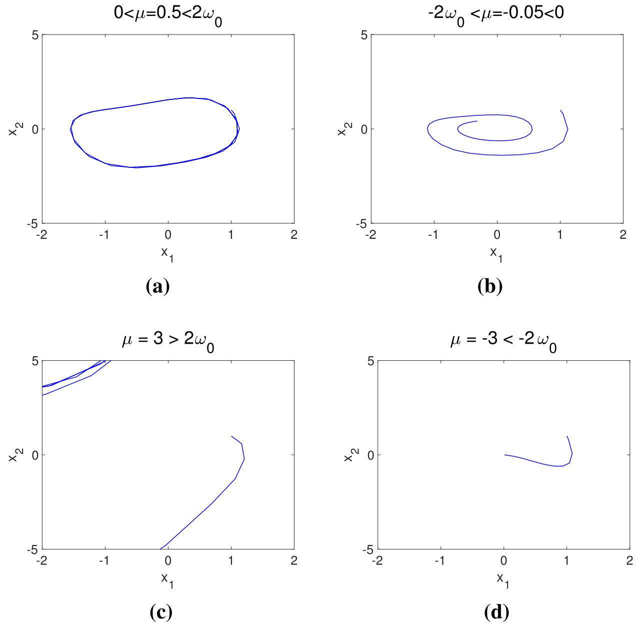

FIGURE 1. The emotion system phase trajectory with different μ.

VI. NUMERICAL SIMULATION AND PROTOTYPE

A. NUMERICAL SIMULATION

In order to analyze the steady-state response of the emotional dynamic system under different environments (with different environmental parameter μ) and the influence of the applied control on the system stability, we first perform the Monte Carlo numerical simulation on the system to verify the theoretical effectiveness.

1) AUTONOMOUS SITUATION

Setting $\omega_0 = 1$ and the initial condition as $x_1 = 1, x_2 = 1$, we can get the phase trajectory of the emotional state vector $\boldsymbol{x}$ without excitations as shown in Fig. 1. Fig. 1(a) indicates that when $0 < \mu = 0.5 < 2\omega_0$, the system is in the Stable State and the phase trajectory quickly approaches the stable limit cycle, which represents a stable periodic solution of the emotional system. From Fig. 1(b) we can see that when $-2\omega_0 < \mu = -0.05 < 0$, the system is in the Gradual Dead State and the emotional state gradually converges to 0 after the amplitude-decreased fluctuation, which means that it is slowly deactivated. Fig. 1(c) means that when $\mu = 3 > 2\omega_0$, the system is in the Explosion State and the emotional state quickly deviates from the equilibrium point, causing the system to crash quickly. As shown in Fig. 1(d), when $\mu = -3 < -2\omega_0$, the system is in the Dead State and the emotional state quickly collapses to 0 resulting in a quickly deactivated system.

The simulation results of the autonomous situation show that different environmental parameters μ can affect the emotional system state. Moreover, with the change of μ, the stability and health status of the emotional system will also change according to the theoretical predictions. This proves the validity of the emotional dynamics model we have established.

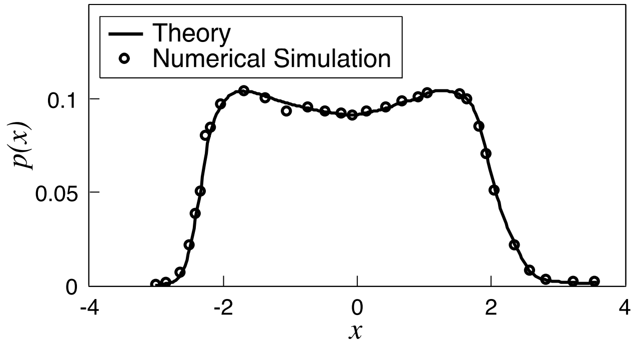

FIGURE 2. Probability density of emotional displacement *x*.

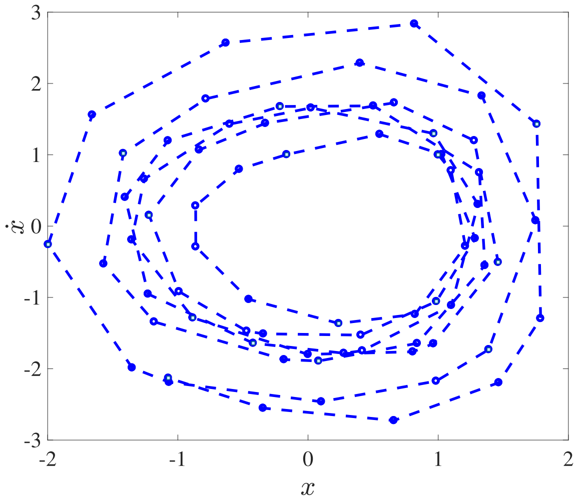

FIGURE 3. Phase trajectory in the case of Gaussian white noise excitation.

2) STOCHASTIC EXCITATION SITUATION

Let $\omega_0 = 1$, $\varepsilon = 0.1$, $\varepsilon^2 2\pi K = 0.01$ and the initial condition is set to $x = 1$, $\dot{x} = 1$. When $\mu = 0.5$, we can get the emotional displacement probability density as shown in Fig. 2 and the phase trajectory of the emotional system under the condition of wideband Gaussian stochastic excitation as shown in Fig. 3. We can see that the emotional displacement x peaks around $x = 2$ and $x = -2$ respectively. Reflected in the phase trajectory, the steady-state response of the system has a diffused limit cycle and the radius on the x axis is close to $r = 2$. The emotional state is in a healthy and stable state with a periodic oscillation. The numerical simulation results in Fig. 2 are very close to the theoretical results, which proves the correctness of our proposed emotional dynamics theory.

In the case of $\mu = 0.5$ above, the system is in a steady state and there is no need to apply external control. Next, we set the environment parameter to $\mu = -0.05$ under the condition that other parameters are unchanged and get the phase trajectory of the system as shown in Fig. 4. We can see that the phase trajectory gradually collapses to the origin and the system state changes to the Gradual Dead State.

If no additional controls are applied to the system, its emotional dynamism will gradually "dead". We enter a feedback control with $k_1 = 0.4$, $k_2 = 0.1$, $E\{x\} = 1.5$ and get the

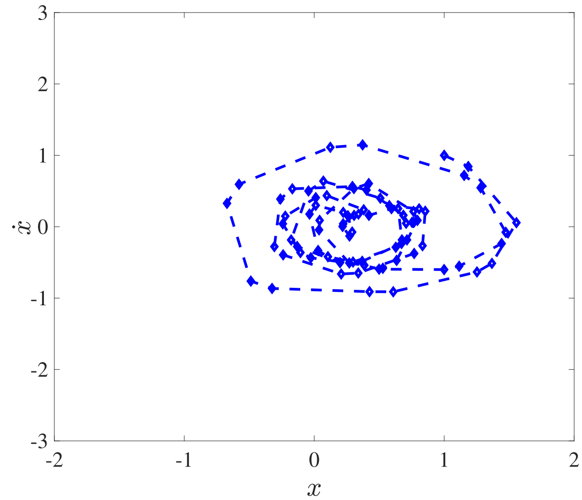

FIGURE 4. Discrete phase trajectory of the uncontrolled system.

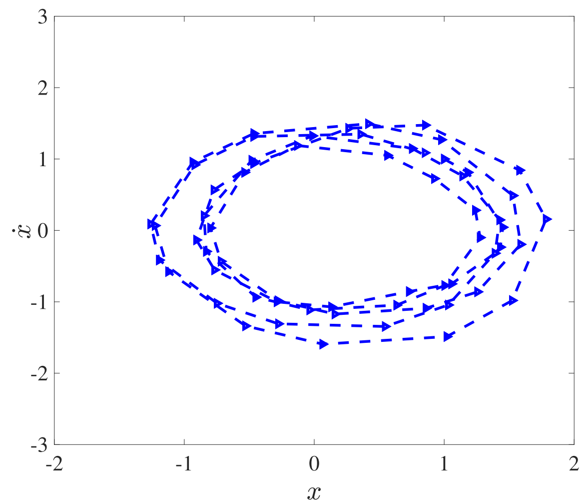

FIGURE 5. Discrete phase trajectory of the controlled system.

phase trajectory of the controlled system as shown in Fig. 5. We can see that the system has a diffusion limit cycle at this time and returns to the Stable State. These results demonstrate the effectiveness of our feedback controller.

B. PROTOTYPE

We also build an application example to apply our proposed emotional dynamics theory and control mechanism to the emotion regulation in human-computer interactions. The experiment is carried out in a closed condition, with the unchanged external environment such as the light and sound. The experimental subjects are played with video clips with different sentiment-directed intensities, e.g. hilarious or horrific movie clips and even video clips that have strong memory associations with the subject (e.g. birthday parties and graduation records). We normalize the emotional strength $x \in \{0, 1\}$ and take $k_1 = 1$, $k_2 = 1$, $\varepsilon = 0.5$, so the control also satisfy $u \in \{0, 1\}$. These video clips are divided into 5 levels $\{0.2, 0.4, 0.6, 0.8, 1.0\}$ according to the

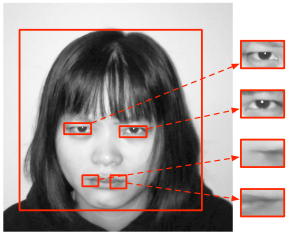

(a) Time unit is 60;
Emotion category is anger;
Emotional intensity: theoretical 1.0 and recognized 0.8.

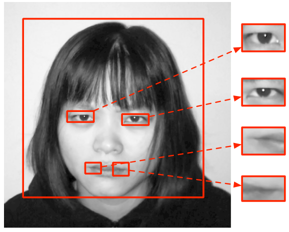

(b) Time unit is 70;
Emotion category is anger;
Emotional intensity: theoretical 0.8 and recognized 0.6.

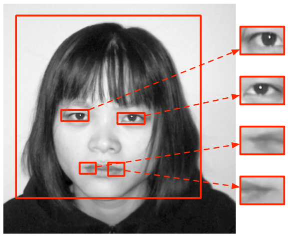

(c) Time unit is 80;
Emotion category is anger;
Emotional intensity: theoretical 0.5 and recognized 0.2.

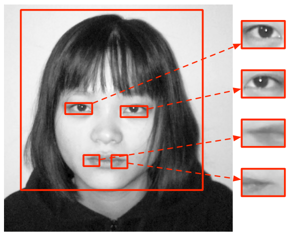

(d) Time unit is 90;
Emotion category is anger;
Emotional intensity: theoretical 0.3 and recognized 0.1.

FIGURE 6. Regulation results of the anger emotion over time.

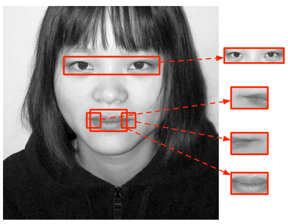

(a) Time unit is 10;
Emotion category is happy;
Emotional intensity: theoretical 0 and recognized 0.2.

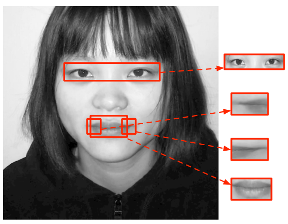

(b) Time unit is 20;
Emotion category is happy;
Emotional intensity: theoretical 0.3 and recognized 0.5.

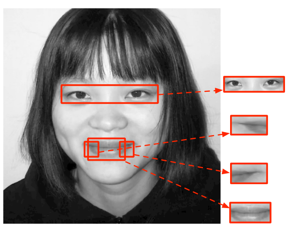

(c) Time unit is 30;
Emotion category is happy;
Emotional intensity: theoretical 0.6 and recognized 0.6.

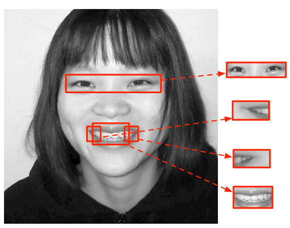

(d) Time unit is 40;
Emotion category is happy;
Emotional intensity: theoretical 0.8 and recognized 1.0.

FIGURE 7. Regulation results of the anger emotion over time.

emotional excitation intensity. We calculate the feedback control quantity according to the emotional dynamics theory to select video clips to achieve the emotional regulation. The emotion recognition of the subject is performed in real time through the facial expression and the recognition results are compared with the theoretical results.

Fig. 6 shows the results of the anger-relieving emotion control experiment. We can see that the anger of the subjects gradually eased after being controlled. And the theoretical values of the anger intensity at 4 moments are not much different from the actual measurement (recognition) value. In fact, the average error of all moments is 27%. This proves that the emotional control mechanism we have established can play a practical role in the mitigation of anger in human-computer interaction. Fig. 7 shows the results of the happy-excitation experiment. We can see that the theoretical values of the happy intensity at 4 moments are similar to the actual measurement (recognition) value. The average error of all moments is 36%, higher than that of the previous experiment but still acceptable. Two sets of experimental results prove that our proposed emotion control mechanism is practical and effective.

VII. CONCLUSION

In this paper we have made full use of the device-side computing power and battery life given by the green IoT and presented a novel emotion control system for embedded human-computer interaction. We first improved the Van der Pol oscillator and equipped it with the nonlinear resilience. Then, we discussed the characteristics of its solution without external excitations. And according to the different orbital stability of the phase trajectory, four health states are defined for the emotional system, including the Stable State, the Gradual Dead State, the Dead State and the Explosion State. Subsequently, we apply the Gaussian white noise as the stochastic incentives usually faced in the real world by the emotional system and use the stochastic averaging method to solve the steady-state solution. Finally, we design a state feedback controller for the emotional system based on the steady-state solution. This makes an emotion-friendly IoT possible and provides a theoretical basis for the more advanced human-computer interaction in the IoT environment.

REFERENCES

[1] D. E. O'Leary, "Artificial intelligence and big data," *IEEE Intell. Syst.*, vol. 28, no. 2, pp. 96–99, Mar./Apr. 2013.

[2] M. Parra-Royon and J. M. Benítez, "Delivering data mining services in cloud computing," in *Proc. IEEE World Congr. Services (SERVICES)*, vol. 2642-939X, Jul. 2019, pp. 396–397.

[3] A. Meloni, P. Pegoraro, L. Atzori, A. Benigni, and S. Sulis, "Cloud-based IoT solution for state estimation in smart grids: Exploiting virtualization and edge-intelligence technologies," *Comput. Netw.*, vol. 130, pp. 156–165, Jan. 2018. [Online]. Available: http://www.sciencedirect.com/science/article/pii/S1389128617303912

[4] M. Maksimovic, "Greening the future: Green Internet of Things (G-IoT) as a key technological enabler of sustainable development," in *Internet of Things and Big Data Analytics Toward Next-Generation Intelligence*. Springer, 2018, pp. 283–313.

[5] Z. Zhou, X. Chen, E. Li, L. Zeng, K. Luo, and J. Zhang, "Edge intelligence: Paving the last mile of artificial intelligence with edge computing," May 2019, *arXiv:1905.10083*. [Online]. Available: https://arxiv.org/abs/1905.10083

[6] F. Lin, Y. Zhou, I. You, J. Lin, X. An, and X. Lü, "Content recommendation algorithm for intelligent navigator in fog computing based IoT environment," *IEEE Access*, vol. 7, pp. 53677–53686, 2019.

[7] F. Song, M. Zhu, Y. Zhou, I. You, and H. Zhang, "Smart collaborative tracking for ubiquitous power IoT in edge-cloud interplay domain," *IEEE Internet Things J.*, to be published.

[8] A. A. Penilla and A. S. Penilla, "Methods and vehicles for capturing emotion of a human driver and moderating vehicle response," U.S. Patent 10 453 453, Oct. 22, 2019.

[9] D. Han, S. Li, and Z. Chen, "Hybrid energy ratio allocation algorithm in a multi-base-station collaboration system," *IEEE Access*, vol. 7, pp. 147001–147009, 2019.
[10] M. M. Hassan, M. G. R. Alam, M. Z. Uddin, S. Huda, A. Almogren, and G. Fortino, "Human emotion recognition using deep belief network architecture," *Inf. Fusion*, vol. 51, pp. 10–18, Nov. 2019.
[11] B. Q. Ford and J. J. Gross, "Why beliefs about emotion matter: An emotion-regulation perspective," *Current Directions Psychol. Sci.*, vol. 28, no. 1, pp. 74–81, 2019.
[12] C. Gong, F. Lin, X. Zhou, and X. Lü, "Amygdala-inspired affective computing: To realize personalized intracranial emotions with accurately observed external emotions," *China Commun.*, vol. 16, no. 8, pp. 115–129, 2019.
[13] H. Hongwen, Z. Chengcheng, X. Shenggang, and F. Lin, "A novel secure data transmission scheme in industrial Internet of Things, China communications," *China Commun.*, vol. 17, no. 1, pp. 73–88, 2020.
[14] S. Li, L. Da Xu, and S. Zhao, "5G Internet of Things: A survey," *J. Ind. Inf. Integr.*, vol. 10, pp. 1–9, Jun. 2018.
[15] V. Sivaraman, H. Gharakheili, C. Fernandes, N. Clark, and T. Karliychuk, "Smart IoT devices in the home: Security and privacy implications," *IEEE Technol. Soc. Mag.*, vol. 37, no. 2, pp. 71–79, Jun. 2018.
[16] B. V. Philip, T. Alpcan, J. Jin, and M. Palaniswami, "Distributed real-time IoT for autonomous vehicles," *IEEE Trans. Ind. Informat.*, vol. 15, no. 2, pp. 1131–1140, Feb. 2019.
[17] F. Lin, Y. Zhou, X. An, I. You, and K. Choo, "Fair resource allocation in an intrusion-detection system for edge computing: Ensuring the security of Internet of Things devices," *IEEE Consum. Electron. Mag.*, vol. 7, no. 6, pp. 45–50, Nov. 2018.
[18] V. Kraaij and N. Garnefski, "The behavioral emotion regulation questionnaire: Development, psychometric properties and relationships with emotional problems and the cognitive emotion regulation questionnaire," *Pers. Individual Differences*, vol. 137, pp. 56–61, Jan. 2019. [Online]. Available: http://www.sciencedirect.com/science/article/pii/S0191886918304318
[19] B. Q. Ford, M. Feinberg, P. Lam, I. B. Mauss, and O. P. John, "Using reappraisal to regulate negative emotion after the 2016 U.S. presidential election: Does emotion regulation trump political action?" *J. Pers. Social Psychol.*, vol. 117, no. 5, pp. 998–1015, 2018.
[20] W. C. Williams, S. A. Morelli, D. C. Ong, and J. Zaki, "Interpersonal emotion regulation: Implications for affiliation, perceived support, relationships, and well-being," *J. Pers. Social Psychol.*, vol. 115, no. 2, p. 224, 2018.
[21] J. D. Elhai, M. F. Tiamiyu, J. W. Weeks, J. C. Levine, K. J. Picard, and B. J. Hall, "Depression and emotion regulation predict objective smartphone use measured over one week," *Pers. Individual Differences*, vol. 133, pp. 21–28, Oct. 2018. [Online]. Available: http://www.sciencedirect.com/science/article/pii/S0191886917303136
[22] N. Haines, Z. Bell, S. Crowell, H. Hahn, D. Kamara, H. McDonough-Caplan, T. Shader, and T. P. Beauchaine, "Using automated computer vision and machine learning to code facial expressions of affect and arousal: Implications for emotion dysregulation research," *Develop. Psychopathol.*, vol. 31, no. 3, pp. 871–886, 2019.
[23] D. Villani, C. Carissoli, S. Triberti, A. Marchetti, G. Gilli, and G. Riva, "Videogames for emotion regulation: A systematic review," *Games Health J.*, vol. 7, no. 2, pp. 85–99, 2018, doi: 10.1089/g4h.2017.0108.
[24] L. F. Bringmann, E. Ferrer, E. L. Hamaker, D. Borsboom, and F. Tuerlinckx, "Modeling nonstationary emotion dynamics in dyads using a time-varying vector-autoregressive model," *Multivariate Behav. Res.*, vol. 53, no. 3, pp. 293–314, 2018.
[25] T. Krone, C. J. Albers, P. Kuppens, and M. E. Timmerman, "A multivariate statistical model for emotion dynamics," *Emotion*, vol. 18, no. 5, p. 739, 2018.
[26] R. Jenke and A. Peer, "A cognitive architecture for modeling emotion dynamics: Intensity estimation from physiological signals," *Cognit. Syst. Res.*, vol. 49, pp. 128–141, Jun. 2018. [Online]. Available: http://www.sciencedirect.com/science/article/pii/S1389041717300220
[27] E. A. Butler, "Interpersonal affect dynamics: It takes two (and time) to tango," *Emotion Rev.*, vol. 7, no. 4, pp. 336–341, 2015.
[28] P. Kuppens and P. Verduyn, "Emotion dynamics," *Current Opinion Psychol.*, vol. 17, pp. 22–26, Oct. 2017. [Online]. Available: http://www.sciencedirect.com/science/article/pii/S2352250X16302019
[29] G. Luong, C. M. Arredondo, and C. Wrzus, "Age differences in emotion regulation dynamics: Anticipatory, reactivity, and recovery processes," in *Emotion Regulation*. Evanston, IL, USA: Routledge, 2018, pp. 226–249.
[30] D. Pincus and A. Metten, "Nonlinear dynamics in biopsychosocial resilience," *Nonlinear Dyn., Psychol., Life Sci.*, vol. 14, no. 4, p. 353, 2010.
[31] S. Vaidyanathan, "Output regulation of the forced Van der Pol chaotic oscillator via adaptive control method," *Int. J. Pharmtech. Res.*, vol. 8, no. 6, pp. 106–116, 2015.
[32] B. D. Hassard, B. Hassard, N. D. Kazarinoff, Y.-H. Wan, and Y. W. Wan, *Theory and Applications of Hopf Bifurcation*, vol. 41. Cambridge, U.K.: Cambridge Univ. Press, 1981.

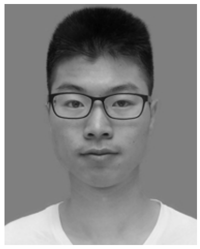

CHAO GONG was born in Shandong, China, in 1990. He received the B.S. degree from the University of Science and Technology Beijing, in 2014, China, where he is currently pursuing the Ph.D. degree with the School of Computer and Communication Engineering. His research interests include affective computing and deep learning.

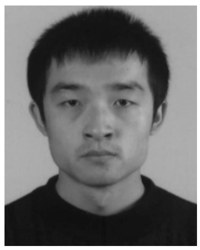

FUHONG LIN received the M.S. and Ph.D. degrees in electronics engineering from Beijing Jiaotong University, Beijing, China, in 2006 and 2010, respectively. He is currently an Associate Professor with the Department of Computer and Communication Engineering, University of Science and Technology Beijing, China. His two articles won top 100 most-cited Chinese articles published in international journals, in 2015 and 2016. His research interests include edge/fog computing, network security, and big data. He received the track Best Paper Award from the IEEE/ACM ICCAD 2017. He won the Provincial and Ministry Science and Technology Progress Award two, in 2017. He served as the Co-Chair of the first and third IET International Conference on Cyberspace Technology and the General Chair of the second IET International Conference on Cyberspace Technology. He was the Leading Editor of the special issue *Recent Advances in Cloud-Aware Mobile Fog Computing* for wireless communications and mobile computing. He currently serves as a Reviewer of more than 10 international journals including the IEEE TRANSACTIONS ON INDUSTRIAL INFORMATICS, IEEE ACCESS, *Information Sciences*, the IEEE INTERNET OF THINGS JOURNAL, *The Computer Journal*, and *China Communications*.

XINGSHUO AN was born in Shandong, China, in 1988. He received the M.S. and Ph.D. degrees from the University of Science and Technology Beijing, in 2014 and 2019, respectively. He is currently engaged in scientific research works with the North China Institute of Computing Technology, China. His research interests include fog computing and network security.